Moroccan Journal of Chemistry
ISSN : 2351-812X

Mor. J. Chem., 2025, Volume 13, Issue 1, Page 248-268
https://revues.imist.ma/index.php/morjchem
https://doi.org/10.48317/IMIST.PRSM/morjchem-v13i1.50230

Isoconversional and DFT Investigation of the Thermal Decomposition of Levofloxacin

Ismail Badran*[1], Mohammed N. Thaher[1]

[1]*Department of Chemistry, Faculty of Sciences, An-Najah National University, Nablus, Palestine*

**For Corresponding author: Email address: i.badran@najah.edu*

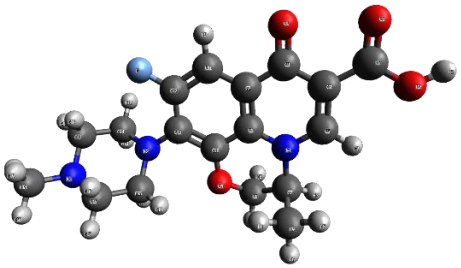

Received *05 July 2024,*
Revised *13 Dec 2024,*
Accepted *15 Dec 2024*

Citation*: Bdran I., Thaher A. O. (2025) Isoconversional and DFT Investigation of the Thermal Decomposition of Levofloxacin, Mor. J. Chem., 13(1), 248-268*

Abstract: Levofloxacin is a widely used fluoroquinolone antibiotic. This study examined the drug using thermogravimetric analysis (TGA) and differential scanning calorimetry (DSC). The study sought to understand the mechanism of the drug's thermal decompaction and its thermal stability and behavior at elevated temperatures for environmental applications. The TGA was done using various heating rates under N2 gas flow. The isoconversional methods of Kissinger-Akahira-Sunose (KAS) and Friedman were used to determine the decomposition's effective activation energy (Eα) based on the extent of conversion (α). The Eα values of levofloxacin's decomposition ranged from 50-120 and 20-70 kJ/mol for KAS and Friedman, respectively. The bond dissociation energies (BDE) of the various levofloxacin degradation routes were calculated using density functional theory (DFT). The experimental results obtained using TGA, DSC, and DFT were used to develop a model for the thermal degradation of the drug, which included a series of heterogeneous reactions.

Keywords: *Sustainability, Isoconversional, kinetics, DFT, Pharmaceutical waste*

1. Introduction

The fate and occurrence of pharmaceutical drugs are critical research areas due to their profound impact on human life and the environment. Amid various aspects, investigating the thermal degradation of these compounds is essential, not only to optimize their product stability and manufacturing processes but also to analyze their degradation products and their impact on human health and ecological systems (Guida, Lanaya, Rbihi, & Hannioui, 2019; Kibuye *et al.*, 2019).

The excessive use of some pharmaceuticals, such as antibiotics, antihistamines, and personal-care products, has exacerbated the presence of pollutants in soil and water, posing serious health risks. This requires the implementation of effective removal methods to separate and eliminate their presence in drinking and irrigation water (Badran, *et al.*, 2020; Couto *et al.*, 2019; Jodeh *et al.*, 2016, Kibuye *et al.*, 2019). In fact, contaminants from pharmaceutical and personal care products (PPCP) have been detected in water samples across the globe (Ebele, Abou-Elwafa Abdallah, & Harrad, 2017; Kibuye *et al.*, 2019; Riyaz & Badran, 2022; Wang & Wang, 2016). The sources of this contamination include human excretion, manufacturing waste, and food wastes. The situation is aggravated by the inability of conventional wastewater treatment plants to effectively remove these contaminants (Couto *et al.*, 2019; Salem *et al.*, 2015). Literature has hinted at the fact that WWTPs are, therefore, neither well-equipped, nor well-designed, enough to remove PPCPs from wastewater (Couto *et al.*, 2019; Riyaz & Badran, 2022). The persistence of PPCPs in water poses a direct threat to organisms relying on the water to live, while some of these products, mainly antibiotic-active pharmaceutical ingredients, also cause the risk of producing antibiotic-resistant bacteria known as "Superbugs" (Honigsbaum, 2018; Riyaz & Badran, 2022).

Levofloxacin (Fig. 1) is a chiral fluoroquinolone antibiotic used to treat a wide range of bacterial infections (Blondeau, 2004). The drug is a hemihydrate in the oral form of the medicine; however, the crystal is subject to polymorphism when grinded, heated and/or treated with different solvents, and produces three different crystal structures (Wei *et al.*, 2019). Levofloxacin was chosen for this study because it is a model molecule of fluoroquinolones, a widely used and multipurpose antibiotics. Previous studies have proven its adverse effects and potential harm to the environment (Thakur et al., 2023; Zhou *et al.*, 2020). Thus, removing this drug from wastewater would significantly and beneficially impact the health and environmental risks caused by its presence in the environment (Blondeau, 2004; Klein *et al.*, 2018; Zhou *et al.*, 2020).

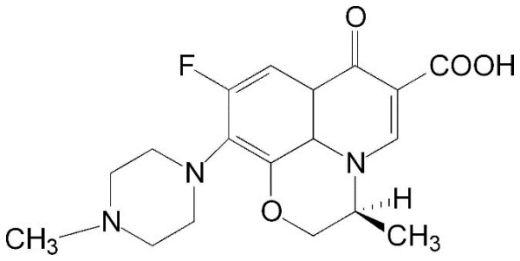

Fig. 1: 2D molecular structure of levofloxacin.

One of the most effective methods used in wastewater treatment is adsorption (Badran & Al-Ejli, 2022; Badran, Al-Ejli, & Nassar, 2023; Manasrah, Montoya, Hassan, & Nassar, 2021; Marzougui et al., 2021; Worch, 2012). This consists of adding an adsorbent to a system of contaminated water, then thermochemically or electrically attaching the waste materials to the adsorbent. While adsorption is considered a highly effective method for treating pollutants, it results in a secondary environmental issue, because, by definition, the process produces solid waste concentrated on the surface of the adsorbent (Badran *et al.*, 2020).

To address this issue, a new technology, known as nanosorbcat, was recently developed which uses the adsorbent as a catalyst for further upgrading of solid waste (Alnajjar *et al.*, 2019; El-Qanni, *et al.*,

2017; El-Qanni, *et al*., 2016). Under certain conditions, including thermal treatment, the nanoadsorbent can catalyze the conversion of solid wastes into useful chemicals or fuel. In this study, we investigated the thermal degradation of levofloxacin to further explore the potentials of nanosorbcat technology. The study also provides insights into levofloxacin degradation pathways and information on its thermal stability and chemical behavior at high temperatures. To achieve these goals, the drug, in its pure form, was analyzed using thermo-gravimetric analysis (TGA) (Al-Zaqri *et al*., 2020; Titi *et al*., 2023; Vyazovkin, 2015; Warad, 2021). and differential scanning calorimetry (DSC) (Menczel & Prime, 2009; Vyazovkin, 2015). These techniques can provide detailed kinetic and thermodynamic parameters that allows constructing a reaction mechanism for organic compounds thermal (under inert atmosphere) or oxidative (under O_2) degradation (Badran, Hassan, Manasrah, & Nassar, 2019; Badran *et al*., 2020; Riyaz & Badran, 2022; Zamani-Babgohari, Irannejad, Khayati, & Kalantari, 2023).

In contrast to the traditional notion of having a single activation energy that correlates to one step, isoconversional kinetics describes the reaction rate ($d\alpha/dt$) as a function of temperature and a reaction model ($f(\alpha)$), which depends on the extent of reaction (α); *(Vyazovkin, 2015)*

$$\frac{d\alpha}{dt} = k(T)f(\alpha) \qquad (1)$$

By using isoconversional kinetic techniques, complex reactions, especially heterogeneous ones, can be described using multi-step kinetic equations. Each equation is associated with a single extent (α) and a narrow temperature range at that extent. This allows for determining different values of the effective activation energy (E_α). Consequently, vital kinetic parameters, such as the entropy ($\Delta S^{\ddagger}$) and enthalpy ($\Delta H^{\ddagger}$) of activations, can be determined (Badran, Hassan, *et al*., 2019; Badran *et al*., 2020; Vyazovkin, 2015; Vyazovkin *et al*., 2011). In this work, the isoconversional methods of Kissinger–Akahira–Sunose (KAS) and Friedman were implemented (Vyazovkin, 2015; Vyazovkin *et al*., 2011; Yuan, He, Cao, & Yuan, 2017).

The reaction mechanism for the thermal degradation of levofloxacin was constructed in the light of Density Functional Theory (DFT) calculations and further supported by experimental results (Al-Ejli, Eribi, Alahzm, & Salih, 2023; Alaoui et al., 2021; Badran, Hashlamoun, & Nassar, 2023; Badran, Hassan, *et al*., 2019; Bouayad et al., 2024; El Azzouzi et al., 2022; Herradi et al., 2024; Kaddouri et al., 2017; Engel, 2011; Manasrah et al., 2017; Parr & Weitao, 1995; Salih, 2021; Vyazovkin, 2015; Warad *et al*., 2017; Weigend & Ahlrichs, 2005; Er-rajy et al., 2023). This work's outcomes align with previous works to construct a model for upgrading materials from waste to potentially beneficial products such as fuels and/or commodity products. (Badran *et al*., 2020; Riyaz & Badran, 2022; Vyazovkin, 2015).

2. Materials and Methods

2.1. Experimental thermochemical analysis

In this research experiment, the temperature dependence of the isoconversional rates of levofloxacin was determined using thermogravimetry using a TGA analyzer (SANAF Co, Turkey). In a typical procedure, approximately 20.0 mg of levofloxacin hemihydrate powder (CAS: 138199-71-0, Sigma Aldrich, MO United States) were heated at different heating rates ranging from 15 - 30 °C/min under N_2. The flow rate was fixed between 65-85 mL/min. The samples heated at a fixed heating rate from

ambient temperature to 800 °C, holding at 110 °C for 10 minutes to allow water evaporation from the sample. The device was set to produce a mass reading every second for the heating period, correlated to a temperature reading at every point.

The TGA device was calibrated beforehand by adjusting for the weight of the appropriate disposable crucible. At that point, the indicated mass of any single run was the mass of the levofloxacin sample. The device was then flushed with N_2 gas to remove any residual particulate matter or residual air from previous runs, and the drug was added in the crucible on the TGA machine's balance compartment.

DSC was performed using the same levofloxacin's sample. The DSC examination was carried using 5.422 mg of levofloxacin hemihydrate. The 'atmosphere' remark denotes the gaseous medium under which the experiment was conducted, N_2 gas at a flow rate between 50.0 ml/min and 60.0ml/min.

2.2. Isoconversional methods

The extent of conversion (α) can be calculated by measuring a given physical property that varies with the reaction's progression (Vyazovkin, 2015; Vyazovkin *et al*., 2011). For this work, the reaction progress was tracked by following the change in levofloxacin's mass using TGA. Therefore, the reaction extent, α, was determined by dividing the incident mass change (Δm) by the total mass change (Δm_{tot}) that has occurred during the entire process (Vyazovkin, 2015; Vyazovkin *et al*., 2011).

$$\alpha = \frac{m_0 - m}{m_0 - m_f} = \frac{\Delta m}{\Delta m_{tot}} \qquad (2)$$

By leveraging the temperature dependence of the isoconversional rate, it becomes possible to estimate the isoconversional activation energy values (E_α) without having to identify or make assumptions about the reaction model (Vyazovkin, 2015; Vyazovkin *et a*l., 2011).

The temperature-dependent rate constant, *k(T)*, is related to the rate and the reaction model by eq. (1). The activation energy as a function of α (E_α) is related to *k(T)* by the Arrhenius equation: (Atkins, De Paula, & Keeler, 2023; Vyazovkin, 2015):

$$k(T) = Ae^{E_\alpha/RT} \qquad (3)$$

where A is the preexponential factor, and R is the universal gas constant. The Isoconversional method employs a unique rate equation for every degree of conversion and a limited temperature range, ΔT, linked to that specific conversion. By utilizing distinct heating rates, (β_1) and (β_2), the approach enables the determination of different rates at the exact conversion, according to the equation (Vyazovkin, 2015; Vyazovkin et al., 2011):

$$\frac{d\alpha}{dt} = ß \left(\frac{d\alpha}{dT}\right) \qquad (4)$$

Therefore, if the aim is to calculate the activation energy, then we plug equation (3) into equation (4) where the temperature dependence would replace the time dependence.:

$$\frac{d\alpha}{dT} = \left(\frac{A_\alpha}{ß}\right) \exp\left(\frac{-E\alpha}{RT}\right) f(\alpha) \qquad (5)$$

After obtaining the temperature dependence of the isoconversional rate via a sequence of temperature programs, and applying the previous equations to the data, it can be parameterized by the differential isoconversional equation given by Friedman: (Friedman, 1969)

$$\ln\left(\frac{d\alpha}{dt}\right)_{\alpha,i} = \ln[A_\alpha f(\alpha)] - \frac{E_\alpha}{RT_{\alpha,i}} \qquad (6)$$

where (i) is the identity number of the temperature program setting for each of the solutions of the equation. The derivative dα/dt is defined as:

$$\frac{d\alpha}{dT} = \frac{-dm/dt}{m_0 - m_f} \qquad (7)$$

Another popular method that is used for the determination of E_α is the Kissinger–Akahira–Sunose (KAS) given by: (Akahira & Sunose, 1971; Kissinger, 1957):

$$ln\left(\frac{\beta_i}{T_{\alpha,i}^2}\right) = \ln\left(-\frac{A_\alpha R}{E_\alpha}\right) - \ln g(\alpha) - \left(\frac{E_\alpha}{RT_{\alpha,i}}\right) \qquad (8)$$

where $g(\alpha)$ is the integral form of the reaction model ($f(\alpha)$). Hence, the effective activation energies can be estimated from the plot of the left side of eq. (8) against $1/T_{\alpha,i}$ at a given α.

Therefore, the activation energy may be calculated from the slope of the best fit line of the plot of ln (ß$\frac{d\alpha}{dt}$) or $ln\left(\frac{\beta_i}{T_{\alpha,i}^2}\right)$ against 1/T(K) at any given α, according to the relation:

$$E_\alpha = \frac{(-slope \times R)}{1000} \qquad (9)$$

The coefficient of regression (R^2) of the plot is then used to assess the goodness of fit for each dataset using Origin Pro. (OriginLab, 2024).

2.3. Theoretical quantum computation

The degradation mechanism of levofloxacin was studied by exploring possible decomposition pathways using DFT methods. First, the structural geometries of the parent levofloxacin and the degradation fragments were optimized using the M06L (Zhao & Truhlar, 2008) functional and the def2-TZVP basis set (Weigend & Ahlrichs, 2005). the optimization was followed by frequency calculation using the same level of theory to characterize the structures' minima. All, the geometry optimizations and frequency calculations, were performed using ORCA 5.0 software (Melo *et al*., 2018; Neese, 2022; Neese, Wennmohs, Becker, & Riplinger, 2020; Sen *et al*., 2018; Stoychev, Auer, Izsák, & Neese, 2018; Stoychev, Auer, & Neese, 2018). and viewed using Avogadro (Hanwell *et al*., 2012).

In this work, several bonds' Bond dissociation energies (BDE) were determined by comparing the potential energy of the anhydrous levofloxacin molecule to the potential energy of the fragments produced by the bond dissociation. Allowing for the determination of the BDE for some of the given bonds, and estimating the most-easily broken bond of the molecule (Atkins *et al*., 2023; Luo, 2007).

The resulting electronic energies were considered single-point energies (SPE), and along with the zero-point energy (ZPE) were used to calculate the enthalpy, entropy and Gibbs free energy at 298K,

400K, and 700K with the temperature command within ORCA 5.0. Herein, the BDE are defined in terms of enthalpy changes as following:

$$\Delta H_{0K} = \left(\sum SPE_{prod.} + ZPE_{Prod.}\right) - (SPE_{react.} + ZPE_{React.}) \quad (10)$$

$$\Delta H_{TK} = \left(\sum SPE_{prod.} + ZPE_{Prod.} + H_{corr.\,TK}\right) - \left(SPE_{react.} + ZPE_{React.} + H_{corr.\,TK}\right) \quad (11)$$

$$\Delta S_{TK} = \left(\sum SPE_{prod.} + ZPE_{Prod.} + S_{corr.\,TK}\right) - \left(SPE_{react.} + ZPE_{React.} + S_{corr.\,TK}\right) \quad (12)$$

$$\Delta G_{TK} = \Delta H_{TK} - \left(\frac{T + \Delta S_{TK}}{1000}\right) \quad (13)$$

where T is the temperature in Kelvin degrees. And each term is used with its corresponding temperature.

The resulting BDE was compared to the energy from the KAS and Friedman methods mentioned previously, to determine the isoconversional method that best correlates to the computational results, and therefore, is the more accurate estimation of the energy value. More details on the theoretical calculations involved in this work is published elsewhere (Badran, Hashlamoun, *et al*., 2023; Badran, Hassan, *et al*., 2019; Badran *et al*., 2020; Badran *et al*., 2022; Er-rajy, El fadili, Faris, Zarougui, & Elhallaoui, 2024).

3. Results and Discussion

3.1. Isoconversional methods using TGA

The thermogram of levofloxacin as obtained by TGA is shown in Fig. 2. The figure depicts the mass loss of the drug upon heating under N_2 gas flow. The drug loses 74.5% of its mass between 220 and 400 °C. This is followed by another loss of 24.5% between 400 – 500 °C. The two mass losses are separated by an overlap region centered at 400 °C, implying a change in the decomposition mechanism. As mentioned in the introduction, the decomposition of organic compounds is a complex solid-state heterogeneous process that may involve multiple bonds breaking and forming simultaneously, with each corresponding to different activation energy. A strong DTG (derivative thermogravimetry) peak has appeared and centered at 320 °C as seen in Fig. 2. The broad nature of the peak supports the complexity of the decomposition. Such behavior is consistent with previous studies on similar molecules (Badran, Hassan, *et al*., 2019; Badran *et al*., 2020; Matos *et al*., 2016; Neglur, Grooff, Hosten, Aucamp, & Liebenberg, 2016; Riyaz & Badran, 2022). The following section will look at the drug's decomposition mechanism and use DFT calculations to explain these mass losses.

It is noteworthy to mention that in their work on the crystallography of levofloxacin, Wei et al. (Wei et al., 2019). and Pereira et al. (Pereira et al., 2015). discussed the polymorphism of levofloxacin and how it affects its degradation. This means that multiple crystal structures could be present or transform differently when exposed to heat. The isoconversional method was used to determine the activation energies of levofloxacin decomposition as detailed in the experimental section. For that purpose, one can consider certain region of the α graph to be the region of interest. The regions should be selected with well-separated thermograms of at least three heating rates (Badran, Hassan, *et al*., 2019; Badran *et al*., 2020; Badran, Manasrah, & Nassar, 2019; Riyaz & Badran, 2022). This work performed the TGA experiments under N_2 (Fig. 2) and air (not shown). The region of interest was considered within

120-550 °C for experiments under N_2, and 115-500 °C for experiments under air. Using these regions, the isoconversional kinetics of the thermal decomposition of levofloxacin was done by applying eq.'s 2-9. The isoconversional curves, represented by the extent of conversion (α) vs/ temperature, are shown for N_2 and air in Fig. 3 and 5, respectively.

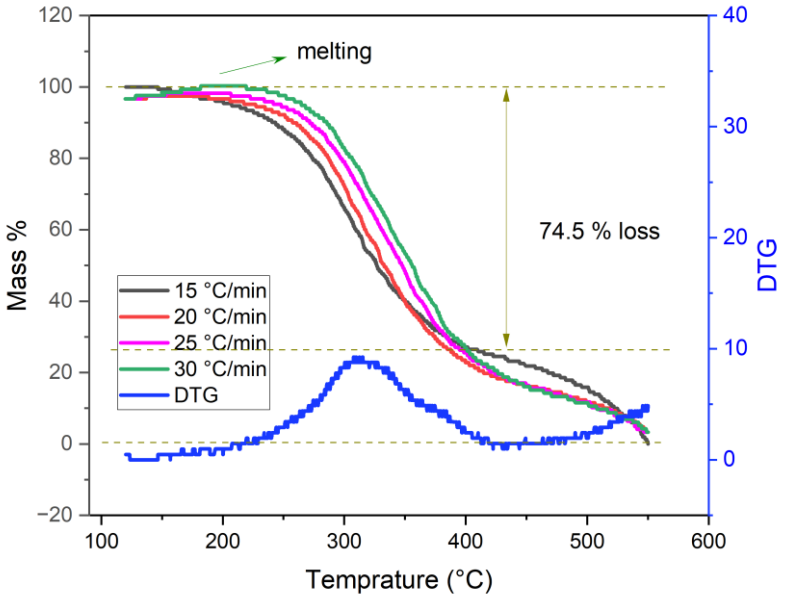

Fig. 2: TGA/DTG thermogram of levofloxacin at different heating rates under N_2 gas, corrected for temperature range between 120-550 °C. (for clarification of the color code of this graph, the reader is referred to the online version of this article).

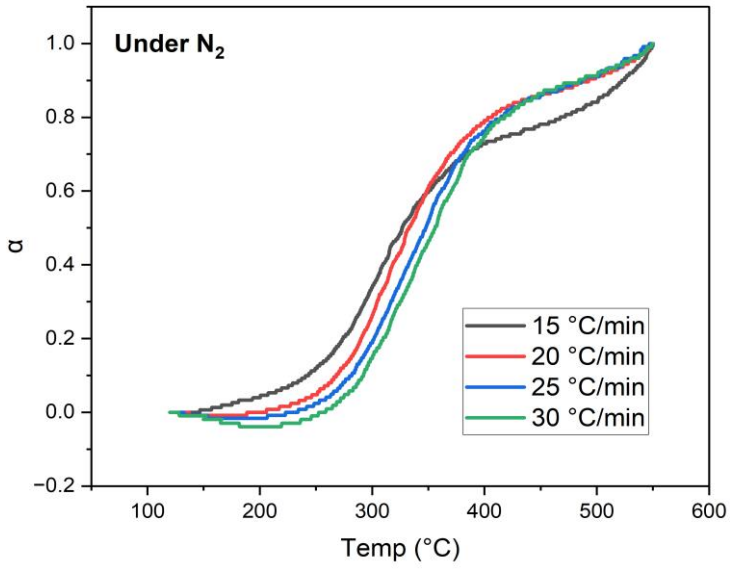

Fig. 3: The extent of conversion (α) as a function of temperature obtained from TGA of levofloxacin hemihydrate at different heating rates under N_2 gas flow of 65-85 mL/min, α graphing corrected for each ß to unify temperature range between 120-550 °C. (for clarification of the color code of this graph, the reader is referred to the online version of this article).

As Fig. 4 shows, the results of experiments under air showed some residual mass at high temperatures. However, in these experiments, no leftover substance was found in the crucible, and the device showed no mass reading after its heating chamber was opened. This phantom mass measurement observed at the higher end of the temperature scaling and the aforementioned discrepancies in the experiments conducted in air are likely a result of the higher pressure exerted by rapid gas formation on the very sensitive mass balance (scale) of the TGA device. This is more evident as the main gases likely to be produced during thermal decomposition under N_2 should be $\bullet CH_3$ radical, or $\bullet NH_2$. radical because of the low concentrations of Oxygen available. However, when Oxygen is present in the reaction environment from the air these gases react to form CO_2 in higher quantities increasing the both the temperature and pressure in the process. For this reason, the results under N_2 condition were selected for further Isoconversional analysis.

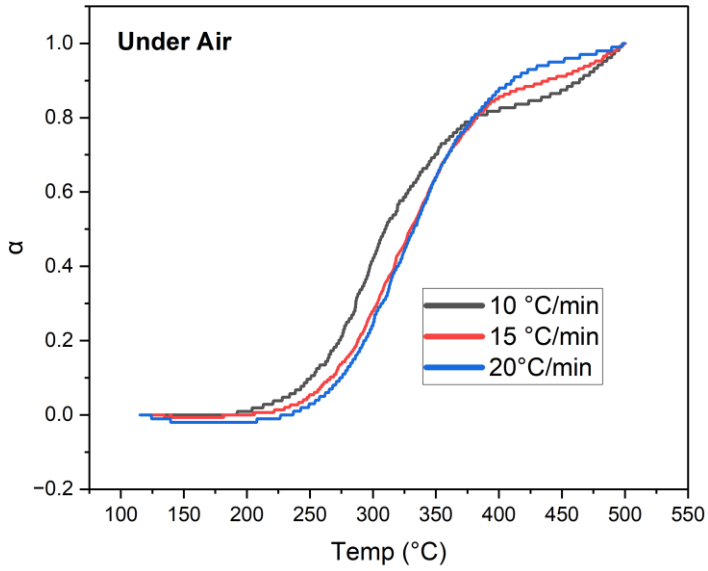

Fig. 4: The extent of conversion (α) as a function of temperature obtained from TGA of levofloxacin at different heating rates under ambient air. α graphing corrected for each ß to unify temperature range between 115-500 °C. (for clarification of the color code of this graph, the reader is referred to the online version of this article).

As shown in Fig. 3, the extend of conversion increases with temperature, and the thermograms at heating rates of 10, 15, and 20 °C/min are well separated in the range of 0.1 – 0.55. Therefore, the methods of Friedman and KAS were implemented in this region and the resulting Arrhenius plots are shown in Fig. 5 and 7. Respectively. The linear fittings based on the Arrhenius equations, eq. 6 and 8, were all acceptable, with regression coefficients (R^2) values above 0.90. The final E_α values of this isoconversional analysis are tabulated in Table 1.

The calculated E_α values were between 28.3 – 114.0 KJ/mol for the Friedman method, and between 9.0 – 61.7 KJ/mol for the KAS method. The E_α values obtained by the Friedman method at $\alpha = 0.65$ are similar to the results approximated by Nisar *et al.*, (Nisar *et al.*, 2020) where they determined the effective activation energy to be 118.05 KJ/mol based on their calculation using Ozawa-Flynn-Wall method (OFW). The effective E_α values obtained from the Friedman and KAS methods are shown in

Fig. 7. The Friedman method produces E_α values ranging between 48 to 117.5 kJ/mol. In contrast, the KAS method produces values between 23 to 69 kJ/mol. Clearly, the values obtained from the KAS method are significantly lower as shown in Fig. 7, which may suggest they are less realistic. In previous studies, the Friedman method was shown to provide E_α values that are more realistic and closer to theoretical values than that of KAS (Badran, Hassan, *et al*., 2019; Badran *et al*., 2020; Badran, Manasrah, *et al*., 2019; Riyaz & Badran, 2022).

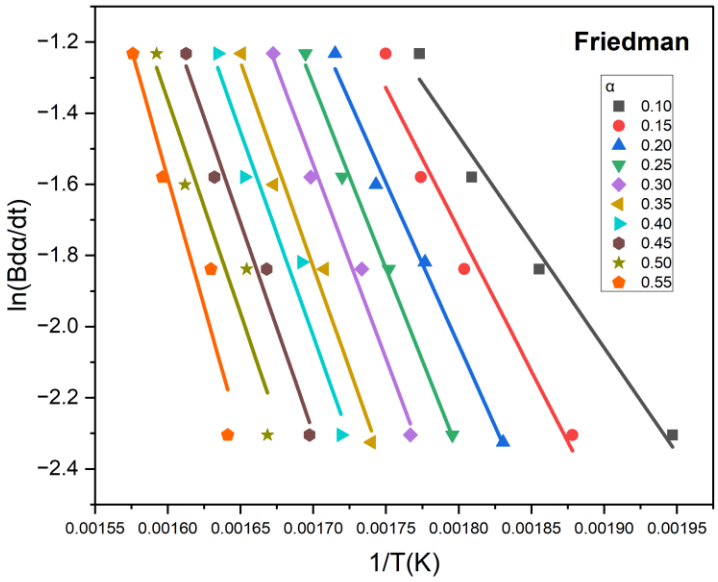

Fig. 5: Linear fittings of the Arrhenius plots for the thermal decomposition of levofloxacin hemihydrate using Friedman method.

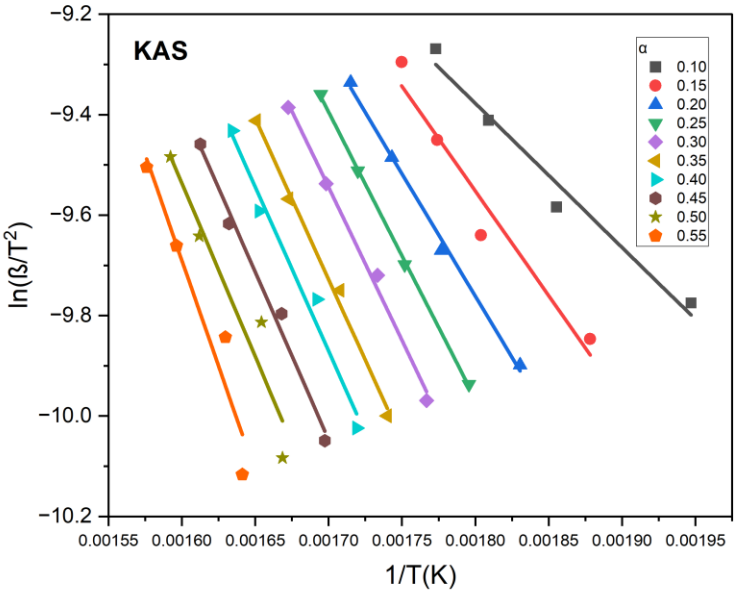

Fig. 6: Linear fittings of the Arrhenius plots for the thermal decomposition of levofloxacin using the KAS method

The relative standard deviation (RSD) of E_α values showed a significant difference between the two methods as illustrated in Fig. 7. The Friedman method produces RSD values between 6.47 to 27.97 kJ/mol. In contrast, the KAS method shows RSD values between 0.03 and 0.17. the figure also demonstrates different E_α values for each α, that is because these points each depict a single moment within a complex reaction mechanism and the polymorphism of the molecule along the reaction mechanism means that there may be several forms of the crystal at each point, with each having a distinct E_α and interaction model (Khawam & Flanagan, 2005; Riyaz & Badran, 2022).

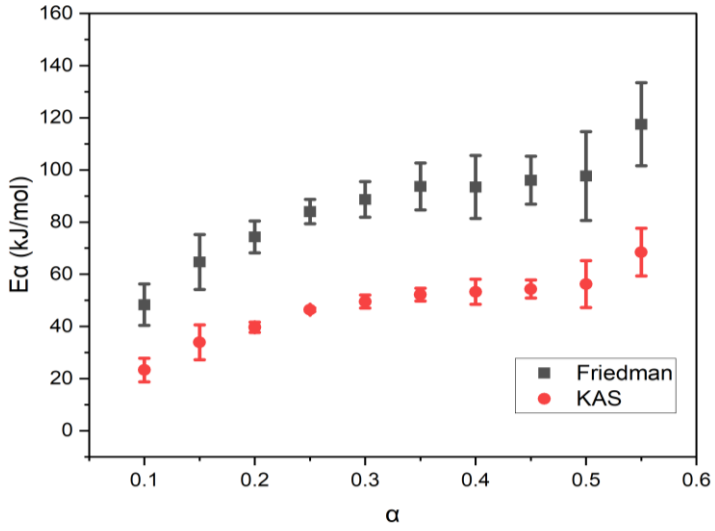

Fig. 7: Effective activation energy (E_α) as a function of α for the thermal decomposition of levofloxacin hemihydrate under N_2 gas, between 120-550 °C, using Friedman and KAS methods. Error bars represent RSD values obtained from at least three trials

Table 1: Results of the Isoconversional analysis of the thermal decomposition of levofloxacin under N_2 gas.

	Friedman				KAS			
α	**slope**	**E_α (KJ/mol)**	**R^2**	**RSD (E_α)**	**slope**	**E_α (KJ/mol)**	**R^2**	**RSD (E_α)**
0.10	-5942.2	48.3	0.98	8.0	-2866.3	23.3	0.97	4.5
0.15	-7956.3	64.7	0.97	10.5	-4168.9	33.9	0.95	6.7
0.20	-9139.5	74.3	0.99	6.1	-4877.9	39.7	1.00	2.0
0.25	-10328.2	84.0	0.99	4.7	-5709.9	46.4	1.00	0.7
0.30	-10905.0	88.7	0.99	6.8	-6089.6	49.5	0.99	2.5
0.35	-11517.7	93.7	0.98	9.0	-6415.8	52.2	0.99	2.5
0.40	-11490.9	93.5	0.95	12.1	-6549.6	53.3	0.98	4.8
0.45	-11810.1	96.1	0.97	9.2	-6677.3	54.3	0.99	3.5
0.50	-12008.1	97.7	0.91	17.1	-6909.7	56.2	0.92	9.0
0.55	-14447.6	117.5	0.92	15.9	-8418.1	68.5	0.92	9.2

The dependence of the E_α on α as shown in Fig. 7 the deviations in E_α values estimated using the Friedman and KAS methods can be explained by the fact that differential isoconversional methods such as Friedman method used in this study are sensitive to experimental noise (Badran *et al.*, 2020).

Additionally, the E_α values obtained by the Friedman method are independent of the heating rate. This gives this method an advantage as it reduces the effects of systematic error in evaluating the activation energy values. This has also been evident in previous works on metformin (13), where they reference further proof from the work of Sbirrazzuoli et al. (Sbirrazzuoli, Girault, & Elégant, 1997) in the simulation of kinetic methods in DSC, where the latter prove the good performance of the Friedman method. As evident in Fig. 7, the E_α is changing, showing an increase with respect to the change in α. This hints at the fact that different experiment steps have different effective activation energies. This is a result of each step probably consisting of a different composition, be it because of stereo chemistry, physical state, or different chemical compounds breaking down or forming withing the reaction apparatus throughout the decomposition steps. This is consistent with the work of previous literature on glimepiride and metformin (Badran *et al*., 2020; Riyaz & Badran, 2022) and shows promise in the consistency of the model to be produced from this kind of experimentation.

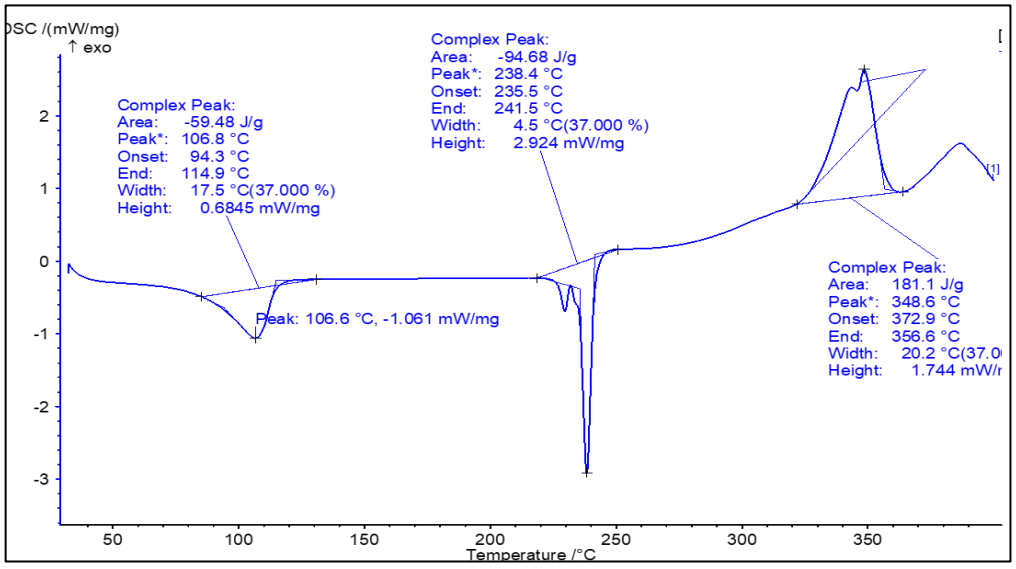

Fig. 8: DSC curve for levofloxacin under N_2 gas flow of 20-60 mL/min,

3.2. DSC results

Fig. 9 shows the DSC curve of levofloxacin under N_2 gas flow. There are three distinct peaks associated with the curve. each of which indicates a certain physical or chemical change. We remember that the area under the curve in DSC corresponds to the heat (q) evolved or absorbed from the reaction. Under constant pressure conditions, this heat will equal ΔH° of the process (Atkins *et al*., 2023). The first peak at 106.8 °C is an endothermic peak that indicates the dehydration of the hemihydrate form of the molecule. This shows that the molecule lost its water content, which is expected when temperatures reach around 100 °C. A small endothermic peak at around 230°C appears next, mostly due to the melting of levofloxacin. The reported melting point of levofloxacin is 227 °C (Nisar *et al*., 2020; Rao, Doodipala, Palem, & Reddy, 2011). This is also consistent with the small TGA/DTG results shown in Fig. 2. The third peak at 238.4 °C is an endothermic peak that corresponds to the dissociation of the molecule. This peak is also shouldering, which means it consists of multiple overlapping peaks, which will be the subject of the next discussion. The fourth peak, 348.6°C, is an exothermic peak. No

oxidation or combustion is expected under pure N_2 flow. So, the only explanation for this peak is the formation of new bonds, which is an exothermic process. At temperatures above 300°C, reactions that produce stable small products, such as the formation of CO_2 CO, N_xO_y, and H_2O, and free-radical recombination reactions, begin to dominate. These reactions involve bond formation, which explains the DSC's negative heat value. Interestingly, the DTG peak in Fig. 2 at 320 °C and the DSC peak at approximately 250 °C coincide. This suggests that, under our circumstances, the formation of stable products actually occurs between 320 and 380 °C.

Compared with the result of Nisar et al. (Nisar et al., 2020), the peaks in Fig. 8 show slight variation in the temperature ranges. However, the flow of heat within the system seems to correspond with the same phenomena; dehydration, melting, and decomposition which resulted in the endothermic peaks in both experiments. On the other hand, Nisar et al. (Nisar *et al.*, 2020) attributed their exothermic complex peak to forming the drug's polymorphs out of the anhydrous form. Since no residues were found at the end of our DSC experiments, we believe that the exothermic peak is the result of stable gaseous molecules formation.

3.3. Theoretical quantum calculations

To better understand levofloxacin thermal degradation, DFT calculations were performed at the M06L/def2-TZVP level of theory, as described in the experimental section. Fig. 9 depicts the drug's degradation mechanism and possible decomposition pathways. The first possible reaction (route a) involves a C-N rupture, resulting in forming two free radical fragments. This route has an estimated standard change in Gibbs energy (ΔG°) of 249.2 kJ/mol. This fragmentation accounts for 27.4 % mass loss from the parent levofloxacin molecule. The next pathway (b) is another C-N bond rupture that yields a methyl radical, accounting for 4.2% mass loss, with an estimated ΔG° of 214.8 k/mol. In pathway (c), a C-C bond breaking leads to the formation of a formyloxyl radical (•COOH), with a mass loss of 12.5%, and an estimated ΔG° of 291.4 kJ/mol. In routes (d) and (e), a fluorine radical and methyl radical form, with mass losses of 5.3% and 4.2%, respectively. The calculated ΔG° for routes (d) and (e) were 354.5 and 225.8 kJ/mol, respectively. This suggests that methyl radical formation is preferable over that of F radical, in agreement with the relative strength of the C-F bond (Luo, 2007).

The calculated ΔG° are all positive, indicating non spontaneous (endergonic) reactions at room temperature (298 K). This makes sense as they all correspond to bond dissociations. This explains why the molecule did not start dissociation below 230 °C as seen from TGA (Fig. 2) and DSC results Fig. 8. Nevertheless, the TGA experiments done on levofloxacin under N_2 flow showed a total mass loss of 74.5% (between 220 -400 °C) as shown in Fig. 2. This mass loss is not consistent with those obtained using DFT calculations (*cf.* Fig. 9).

The cause of the 74.5% mass loss remains unknown. To answer this question, we repeated the calculations at higher temperatures (400K and 700K) to get closer to the environmental conditions of our experiment. The ΔG° values obtained at 298, 400, and 700 K are tabulated for the five reaction routes in Table 2. The values of the changes in enthalpy (ΔH°) and entropy (ΔS°) are also tabulated for reference. The values of ΔH° are all positive (endothermic), due to the energy required to break the bonds. The ΔS° values are all positive due to the increase in translational entropy associated with the formation of two free radical fragments out of one single molecule. This positive values of both ΔH°

and ΔS° leads to a decrease in ΔG° as temperature increases, in accordance with the principles of thermodynamics (ΔG°= ΔH°- TΔS°). In fact, some ΔG° turns negative at elevated temperatures as shown in Table 2.

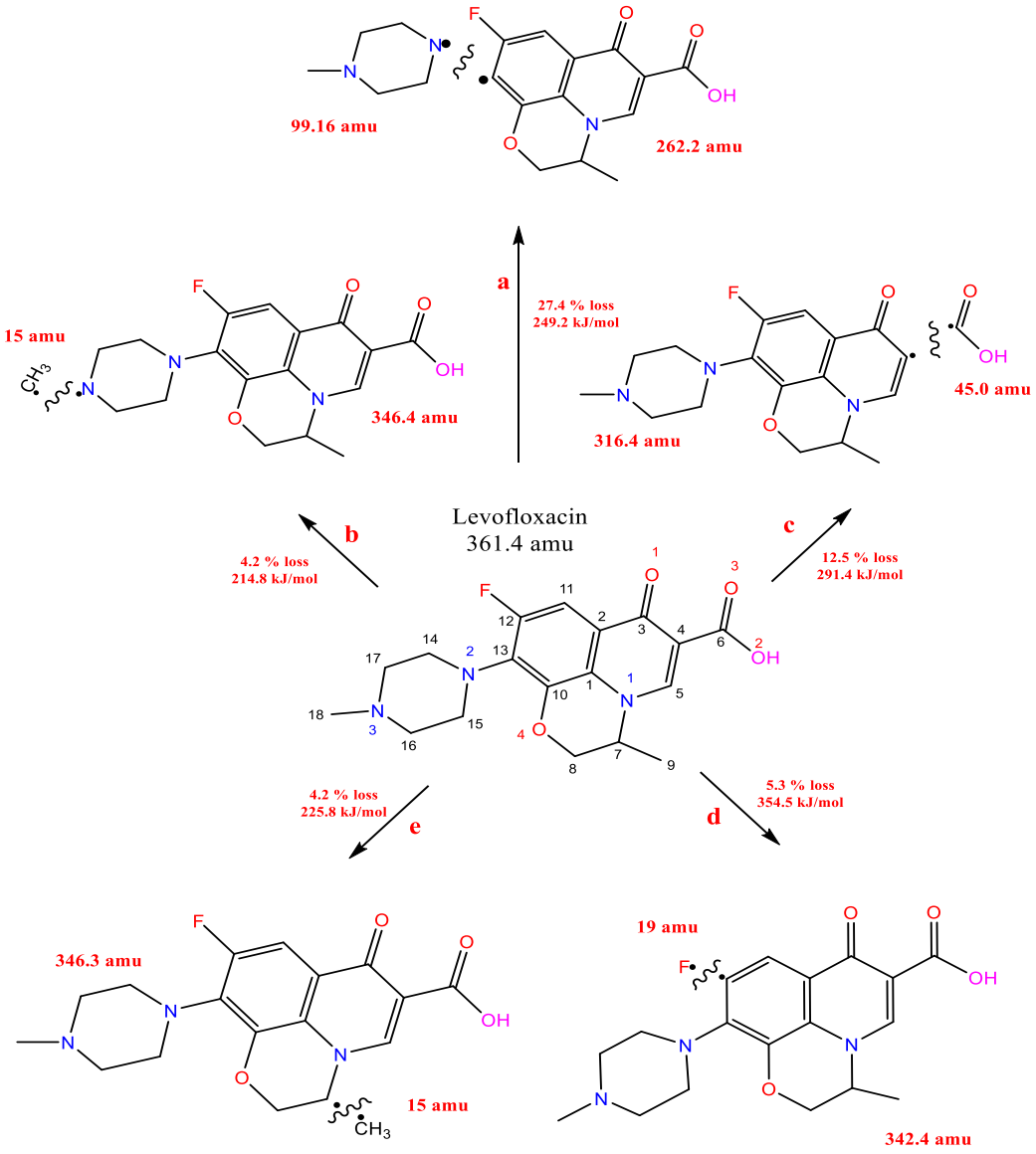

Fig. 9: Expected bond dissociations of levofloxacin as explored at M06L/def2-TZVP level of theory. Energy values represent Gibbs free energies at 298K.

At 700 K (427°C), the ΔG° data differs from those obtained at room temperature, yielding intriguing results. The ΔG° values for routes (b) and (e) are exergonic at 700 K with values of -160.9 and 167.2 kJ/mol. These routes correspond to the formation of methyl radicals. Therefore, we infer that the formation of methyl radicals is the most favorable pathway in levofloxacin's thermal decomposition. Losing a methyl radical causes smaller fragments (routes b and e) to form, which can then be degraded further, resulting in more mass losses in a chain degradation mechanism. This can answer the large mass loss of 74.5% shown in Fig. 2. This finding suggests that multiple reactions are taking place within this temperature range in our experiments, and provides an explanation to the different values of activation energies obtained from our isoconversional kinetic analysis (*cf.* Fig. 7)

Table 2: Theoretical quantum computation calculations' results for each fragment of levofloxacin, at 298K, 400K, 700K.

Levofloxacin

	Route a			Route b			Route c		
Temp.	**298K**	**400K**	**700K**	**298K**	**400K**	**700K**	**298K**	**400K**	**700K**
ΔH° (KJ/mol)	384.8	384.4	382.2	328.9	371.3	549.2	441.5	482.8	839.5
ΔS° (J/K.mol)	454.8	480.7	557.2	382.7	512.3	1014.5	503.7	634.3	1140.3
ΔG° (KJ/mol)	249.2	192.1	-7.8	214.8	166.4	-160.9	291.4	229.1	41.3
	Route d			Route e					
Temp.	**298K**	**400K**	**700K**	**298K**	**400K**	**700K**			
ΔH° (KJ/mol)	505.3	546.2	721.4	347.1	391.3	573.9			
ΔS° (J/K.mol)	506.2	612.5	1045.0	406.7	541.2	1058.8			
ΔG° (KJ/mol)	354.5	301.2	-10.0	225.8	174.8	-167.2			

Now we compare the results obtained from the theoretical calculations to the experimental E_α obtained using isoconversional analysis. The values ranged between 20 – 70 kJ/ mol for KAS, and 50 – 120 kJ/mol for FR (see Fig. 7). However, the theoretical the ΔH° and the ΔG° were much higher (Table 2). This difference can be explained by several factors, first, the theoretical ΔG° values were calculated at ambient conditions (25°C and 1 bar) in the gas phase, but the thermal degradation of levofloxacin takes place at higher temperature and involve complex heterogenies reactions. When the ΔG° values were re-calculated at higher temperature, we notice a dramatic decrease in their values due to the increase in entropy. Since the activation energy of reaction can be represented as the change in the Gibbs free energy of activation (Atkins *et al*., 2023), we can see that ΔG° values at elevated temperatures are closer to the experimental E_α than at room temperature (Badran *et al*., 2020).

Conclusion

The thermodynamics and kinetics of the thermal decompaction of levofloxacin were investigated using TGA, DSC, and isoconversional methods. The study revealed that the decompaction starts with a rapid melting at 230 °C, followed by a large mass loss of 74.5 % between 220 and 400 °C, before the drugs completely decompose at 500 °C.

The isoconversional methods of KAS and Friedman were used to deduce the effective activation energies of the decomposition. The estimated E_α values of the experiments under N_2 were in the range of 50 – 120 and 20-70 kJ/mol for KAS and Friedman, respectively.

Although the large mass loss of 74.5 % sees as a single process in the TGA, the results obtained from DSC and the isoconversional analysis revealed that the decomposition process involves a multistep mechanism which explained the variation of E_α values during the experiment.

DFT calculations using the M06L functional and the def2-TZVP basis set were used to investigate the potential decomposition routes of levofloxacin. We investigated five different decomposition routes and calculated bond dissociation energies in terms of ΔH°. Using frequency calculations, the corresponding values of ΔS° and ΔG° were also calculated. The calculations were done at ambient temperature as well as 400 and 700 K. The room-temperature BDE values obtained

using DFT did not match the experimental E_α values. However, those obtained at elevated temperatures were closer to the experimental E_α.

TGA, DSC, and DFT results were used to construct a reaction mechanism. The mechanism does not involve oxidation because the reactions were carried out under N_2 flow. In the first phase, between 220 and 400 °C, the reaction proceeds by losing methyl radicals, which contains the weakest bonds, followed by further molecule fragmentation, resulting in a large mass loss of 74.5%. This phase is characterized by endothermic peaks in the DSC thermogram. This is followed by a second phase at temperatures above 400 °C. The reactions are then dominated by free radical recombination and the formation of small stable molecules, as indicated by exothermic peaks in the DSC.

Finally, it is recommended that these findings be expanded upon for potential engineering and environmental solutions. Based on analyses such as the method used in this work, and particularly the WTE upgrading potential, such analyses provide the practical data that nanosorbcats technology requires to be beneficially applied to reduce environmental risks associated with PPCPs while also eliminating the secondary waste issue of conventional WWTPs.

Ethics approval and consent to participate

Not applicable

Consent for publication: Not applicable

Availability of data and materials

The raw data required to reproduce these findings are available upon request from the corresponding author at i.badran@najah.edu

Author's contribution

The authors confirm contribution to the paper as follows: study conception and design: Badran, theoretical calculations and modeling: Thaher; data analysis: Thaher, Data validation: Badran, draft manuscript preparation: Thaher, Badran. All authors reviewed the results and approved the final version of the manuscript.

Funding: Not applicable

Conflicts of interest: The authors declare that there is no conflict of interest regarding the publication of this article

Acknowledgements: The authors would like to thank the department of chemistry at An-Najah University for making their facilities and staff available, and for their continuous guidance. Especially Mr. Ameed Amireh and Dr. Murad Abualhasan for providing technical laboratory assistance. A token of gratitude goes out to the University of Jordan for assisting the experimental analysis.

References

Akahira, T, & Sunose, T. (1971). Method of determining activation deterioration constant of electrical insulating materials. *Res Rep Chiba Inst Technol (Sci Technol), 16*(1971), 22-31.

Al-Ejli, M. O., Eribi, Abubaker, Alahzm, Abdulrhman M., & Salih, Kifah S. M. (2023). Synthesis, structural elucidation and optical activity of symmetric Schiff base-functionalized ferrocenes: Synergetic experimental and DFT insights. *Journal of Molecular Structure, 1280*, 135052. https://doi.org/10.1016/j.molstruc.2023.135052

Alaoui, Y, El Moudane, M, Er-Rafai, A, Khachani, M, et al. (2021). Structural study, thermal and physical properties of K_2O-CaO-P_2O_5 phosphate glasses. *Moroccan Journal of Chemistry*, 9(3), 2454-2463. https://doi.org/10.48317/IMIST.PRSM/morjchem-v9i2.22505

Al-Zaqri, N., Khatib, Tamer, Alsalme, Ali, Alharthi, Fahad A., Zarrouk, A. & Warad, I. (2020). Synthesis and amide imidic prototropic tautomerization in thiophene-2-carbohydrazide: XRD, DFT/HSA-computation, DNA-docking, TG and isoconversional kinetics via FWO and KAS models. *RSC Advances, 10*(4), 2037-2048. https://doi.org/10.1039/C9RA09831C

Alnajjar, M., Hethnawi, A., Nafie, Ghada, Hassan, Azfar, Vitale, G., & Nassar, N. N. (2019). Silica-alumina composite as an effective adsorbent for the removal of metformin from water. *Journal of Environmental Chemical Engineering, 7*(3), 102994. https://doi.org/10.1016/j.jece.2019.102994

Atkins, Peter William, De Paula, Julio, & Keeler, James. (2023). *Atkins' physical chemistry*: Oxford university press.

Badran, Ismail, & Al-Ejli, Maan O. (2022). Efficient Multi-walled Carbon Nanotubes/Iron Oxide Nanocomposite for the Removal of the Drug Ketoprofen for Wastewater Treatment Applications. *ChemistrySelect, 7*(38), e202202976. https://doi.org/10.1002/slct.202202976

Badran, Ismail, Al-Ejli, Maan Omar, & Nassar, Nashaat N. (2023). 2 - Applications of nanomaterials for adsorptive removal of various pollutants from water bodies. In Chaudhery Mustansar Hussain & Nashaat N. Nassar (Eds.), *Nanoremediation* (pp. 25-62): Elsevier. https://doi.org/10.1016/B978-0-12-823874-5.00006-1

Badran, Ismail, Hashlamoun, Kotaybah, & Nassar, Nashaat N. (2023). Bond dissociation energies of the fifth-row elements (In□I): A quantum theoretical benchmark study. *International Journal of Quantum Chemistry, 123*(23), e27222. https://doi.org/10.1002/qua.27222

Badran, Ismail, Hassan, Azfar, Manasrah, Abdallah D., & Nassar, Nashaat N. (2019). Experimental and theoretical studies on the thermal decomposition of metformin. *Journal of Thermal Analysis and Calorimetry, 138*(1), 433-441. https://doi.org/10.1007/s10973-019-08213-9

Badran, Ismail, Manasrah, Abdallah D., Hassan, Azfar, & Nassar, Nashaat N. (2020). Kinetic study of the thermo-oxidative decomposition of metformin by isoconversional and theoretical methods. *Thermochimica Acta, 694*, 178797. https://doi.org/10.1016/j.tca.2020.178797

Badran, Ismail, Manasrah, Abdallah D., & Nassar, Nashaat N. (2019). A combined experimental and density functional theory study of metformin oxy-cracking for pharmaceutical wastewater treatment. *RSC Advances, 9*(24), 13403-13413. https://doi.org/10.1039/C9RA01641D

Badran, Ismail, Sahar Riyaz, Najamus, Shraim, Amjad M., & Nassar, Nashaat N. (2022). Density functional theory study on the catalytic dehydrogenation of methane on MoO_3 (010) surface. *Computational and Theoretical Chemistry, 1211*, 113689. https://doi.org/10.1016/j.comptc.2022.113689

Blondeau, Joseph M. (2004). Fluoroquinolones: mechanism of action, classification, and development of resistance. *Survey of Ophthalmology, 49*(2, Supplement 2), S73-S78. https://doi.org/10.1016/j.survophthal.2004.01.005

Bouayad, A, Zerrouk, M, Salim, R, Er-rajy, M, Raza, A, Azzaoui, K, . . . Lachkar, M. (2024). Ba (H_2PO_3) 2.0. $5H_2O$: Synthesis, crystal structure optimization, vibrational study, DFT computation and application as a corrosion inhibitor. *Moroccan Journal of Chemistry*, 12(4), 1575-1595. https://doi.org/10.48317/IMIST.PRSM/morjchem-v12i4.50321

Couto, Carolina F., Lange, Lisete C., & Amaral, Miriam C.S. (2019). Occurrence, fate and removal of pharmaceutically active compounds (PhACs) in water and wastewater treatment plants—A review. *Journal of Water Process Engineering, 32*, 100927. https://doi.org/10.1016/j.jwpe.2019.100927

Cramer, Christopher J. (2013). *Essentials of computational chemistry: theories and models*: John Wiley & Sons.

Ebele, Anekwe Jennifer, Abou-Elwafa Abdallah, Mohamed, & Harrad, Stuart. (2017). Pharmaceuticals and personal care products (PPCPs) in the freshwater aquatic environment. *Emerging Contaminants, 3*(1), 1–16. https://doi.org/10.1016/j.emcon.2016.12.004

El Azzouzi, M, Azzaoui, K, Warad, I, Hammouti, B, Shityakov, S, Sabbahi, R, . . . Jodeh, S. (2022). Moroccan, Mauritania, and senegalese gum Arabic variants as green corrosion inhibitors for mild steel in HCl: Weight loss, electrochemical, AFM and XPS studies. *Journal of Molecular Liquids*, 347, 118354. https://doi.org/10.1016/j.molliq.2021.118354

Er-rajy, Mohammed, El fadili, Mohamed, Faris, Abdelmoujoud, Zarougui, Sara, & Elhallaoui, Menana. (2024). Design of potential anti-cancer agents as COX-2 inhibitors, using 3D-QSAR modeling, molecular docking, oral bioavailability proprieties, and molecular dynamics simulation. *Anti-Cancer Drugs*, 35(2), 117-128. https://doi.org/10.1097/cad.0000000000001492.

Er-rajy, Mohammed, El fadili, Mohamed, Imtara, Hamada, Saeed, Aamir, Ur Rehman, Abid, Zarougui, Sara, . . . Elhallaoui, Menana. (2023). 3D-QSAR Studies, Molecular Docking, Molecular Dynamic Simulation, and ADMET Proprieties of Novel Pteridinone Derivatives as PLK1 Inhibitors for the Treatment of Prostate Cancer. *Life*, 13(1), 127. https://doi.org/10.3390/life13010127

El-Qanni, Amjad, Nassar, Nashaat N., & Vitale, Gerardo. (2017). A combined experimental and computational modeling study on adsorption of propionic acid onto silica-embedded NiO/MgO nanoparticles. *Chemical Engineering Journal*, *327*, 666-677. https://doi.org/10.1016/j.cej.2017.06.126

El-Qanni, Amjad, Nassar, Nashaat N., Vitale, Gerardo, & Hassan, Azfar. (2016). Maghemite nanosorbcats for methylene blue adsorption and subsequent catalytic thermo-oxidative decomposition: Computational modeling and thermodynamics studies. *Journal of Colloid and Interface Science, 461*, 396-408. https://doi.org/10.1016/j.jcis.2015.09.041

Engel, Eberhard. (2011). *Density functional theory*: Springer.

Friedman, Henry L. (1969). New methods for evaluating kinetic parameters from thermal analysis data. *Journal of Polymer Science Part B: Polymer Letters, 7*(1), 41-46. https://doi.org/10.1002/pol.1969.110070109

Guida, MY, Lanaya, S, Rbihi, Z, & Hannioui, A. (2019). Thermal degradation behaviors of sawdust wood waste: pyrolysis kinetic and mechanism. *J. Mater. Environ. Sci*, 10(8), 742-755.

Hanwell, Marcus D., Curtis, Donald E., Lonie, David C., Vandermeersch, Tim, Zurek, Eva, & Hutchison, Geoffrey R. (2012). Avogadro: an advanced semantic chemical editor, visualization, and analysis platform. *Journal of Cheminformatics, 4*(1), 17. https://doi.org/10.1186/1758-2946-4-17

Herradi, S, Adouar, I, Zerrouk, M, Bouhazma, S, Omari, M EL, Ouarsal, R, . . . Lachkar, M. (2024). Physicochemical study of magnesium zinc codoped-hydroxyapatite. *Moroccan Journal of Chemistry*, 12(3), 1240-1253. https://doi.org/10.48317/IMIST.PRSM/morjchem-v12i3.48113

Honigsbaum, Mark. (2018). Superbugs and us. *The Lancet, 391*(10119), 420. https://doi.org/10.1016/S0140-6736(18)30110-7

Jodeh, S, Amarah, J, Radi, S, Hamed, O, Warad, I, Salghi, Alkowni, R. (2016). Removal of methylene blue from industrial wastewater in Palestine using polysiloxane surface modified with

bipyrazolic tripodal receptor. *Moroccan Journal of Chemistry*, 4(1), 2140-2156. https://doi.org/10.48317/IMIST.PRSM/morjchem-v4i1.4015

Kaddouri, Y, Takfaoui, A, Abrigach, F, El Azzouzi, M, Zarrouk, A, El-Hajjaji, F, . . . Sdassi, H. (2017). Tridentate pyrazole ligands: synthesis, characterization and corrosion inhibition properties with theoretical investigations. J. Mater. Environ. Sci, 8(3), 845-856.

Khawam, Ammar, & Flanagan, Douglas R. (2005). Role of isoconversional methods in varying activation energies of solid-state kinetics: II. Nonisothermal kinetic studies. *Thermochimica Acta, 436*(1), 101-112. https://doi.org/10.1016/j.tca.2005.05.015

Kibuye, Faith A., Gall, Heather E., Elkin, Kyle R., Ayers, Brittany, Veith, Tamie L., Miller, Megan, . . . Elliott, Herschel A. (2019). Fate of pharmaceuticals in a spray-irrigation system: From wastewater to groundwater. *The Science of the total environment, 654*, 197–208. https://doi.org/10.1016/j.scitotenv.2018.10.442

Kissinger, Homer E. (1957). Reaction kinetics in differential thermal analysis. *Analytical chemistry, 29*(11), 1702-1706. http://doi.org/10.1021/ac60131a045

Klein, Eili Y., van Boeckel, Thomas P., Martinez, Elena M., Pant, Suraj, Gandra, Sumanth, Levin, et al. (2018). Global increase and geographic convergence in antibiotic consumption between 2000 and 2015. *Proceedings of the National Academy of Sciences of the United States of America, 115*(15), E3463-E3470. https://doi.org/10.1073/pnas.1717295115

Luo, Yu-Ran. (2007). *Comprehensive handbook of chemical bond energies*: CRC press.

Manasrah, Abdallah D., El-Qanni, Amjad, Badran, Ismail, Carbognani Ortega, Lante, Perez-Zurita, M. Josefina, & Nassar, Nashaat N. (2017). Experimental and theoretical studies on oxy-cracking of Quinolin-65 as a model molecule for residual feedstocks. *Reaction Chemistry & Engineering, 2*(5), 703-719. https://doi.org/10.1039/C7RE00048K

Manasrah, Abdallah D., Montoya, Tatiana, Hassan, Azfar, & Nassar, Nashaat N. (2021). Nanoparticles as Adsorbents for Asphaltenes. In Nashaat N. Nassar, Farid B. Cortés, & Camilo A. Franco (Eds.), *Nanoparticles: An Emerging Technology for Oil Production and Processing Applications* (pp. 97-129). Cham: Springer International Publishing. https://doi.org/10.1007/978-3-319-12051-5_3

Marzougui, Zied, Damak, Mohamed, Chaari, Leila, Ghrab, Sana, Elaissari, Abdelhamid, & Elleuch, Boubaker. (2021, 2021//). *Iron Removal from Groundwater by Adsorption Process onto Activated Carbon Obtained from Pinus Halepensis Cone Wastes.* Paper presented at the Recent Advances in Environmental Science from the Euro-Mediterranean and Surrounding Regions (2nd Edition), Cham.

Matos, J., Oliveira, J. F., Magalhães, D., Dubaj, T., Cibulková, Z., & Šimon, P. (2016). Kinetics of ambuphylline decomposition studied by the incremental isoconversional method. *Journal of Thermal Analysis and Calorimetry, 123*(2), 1031-1036. https://doi.org/10.1007/s10973-015-4899-z

Melo, Marcelo C. R., Bernardi, Rafael C., Rudack, Till, Scheurer, Maximilian, Riplinger, Christoph, Phillips, James C., . . . Luthey-Schulten, Zaida. (2018). NAMD goes quantum: an integrative suite for hybrid simulations. *Nature Methods, 15*(5), 351-354. https://doi.org/10.1038/nmeth.4638

Menczel, Joseph D., & Prime, R. Bruce. (2009). *Thermal analysis of polymers: Fundamentals and applications*. Hoboken N.J.: John Wiley.

Neese, Frank. (2022). Software update: The ORCA program system—Version 5.0. *WIREs Computational Molecular Science, 12*(5), e1606. https://doi.org/10.1002/wcms.1606

Neese, Frank, Wennmohs, Frank, Becker, Ute, & Riplinger, Christoph. (2020). The ORCA quantum chemistry program package. *The Journal of Chemical Physics, 152*(22). https://doi.org/10.1063/5.0004608

Neglur, R., Grooff, D., Hosten, E., Aucamp, M., & Liebenberg, W. (2016). Approximation-based integral versus differential isoconversional approaches to the evaluation of kinetic parameters from thermogravimetry. *Journal of Thermal Analysis and Calorimetry, 123*(3), 2599-2610. https://doi.org/10.1007/s10973-016-5244-x

Nisar, Jan, Iqbal, Mudassir, Iqbal, Munawar, Shah, Afzal, Akhter, Mohammad Salim, Sirajuddin, . . . Khan, Muhammad Sufaid. (2020). Decomposition Kinetics of Levofloxacin: Drug-Excipient Interaction. *Zeitschrift für Physikalische Chemie, 234*(1), 117-128. https://doi.org/10.1515/zpch-2018-1273

OriginLab. (2024). Origin: Scientific Data Analysis and Graphing Software (Version 2024): OriginLab. Retrieved from ww.OriginLab.com

Parr, Robert G, & Weitao, Yang. (1995). *Density-Functional Theory of Atoms and Molecules*: Oxford University Press.

Pereira, Rafael Nicolay, Fandaruff, Cinira, Riekes, Manoela Klüppel, Monti, Gustavo A., de Campos, Carlos Eduardo Maduro, Cuffini, Silvia Lucia, & Silva, Marcos Antonio Segatto. (2015). Grinding effect on levofloxacin hemihydrate. *Journal of Thermal Analysis and Calorimetry, 119*(2), 989-994. https://doi.org/10.1007/s10973-014-4233-1

Rao, Yamsani Madhusudan, Doodipala, Narender, Palem, Chinna Reddy, & Reddy, S. Srikanth. (2011). *Pharmaceutical Development and Clinical Pharmacokinetic Evaluation of Gastroretentive Floating Matrix Tablets of Levofloxacin*.

Riyaz, Najamus Sahar, & Badran, Ismail. (2022). The catalytic thermo-oxidative decomposition of glimepiride using the isoconversional method. *Journal of Thermal Analysis and Calorimetry, 147*(19), 10755-10765. https://doi.org/10.1007/s10973-022-11304-9

Salem B. S., Mezni M., Errami M., Amine K.M., Salghi R., Ali. Ismat H., Chakir A., Hammouti B., Messali M., Fattouch S. (2015), Degradation of Enrofloxacin Antibiotic under Combined Ionizing Radiation and Biological Removal Technologies, *Int. J. Electrochem. Sci.*, 10 N°4, 3613-3622, https://doi.org/10.1016/S1452-3981(23)06565-3

Salih, Kifah S. M. (2021). Synthesis, characterization, surface analysis, optical activity and solvent effects on the electronic absorptions of Schiff base-functionalized amino thiophene derivatives: Experimental and TD-DFT investigations. *Journal of Molecular Structure, 1244*, 131267. https://doi.org/10.1016/j.molstruc.2021.131267

Sbirrazzuoli, N., Girault, Y., & Elégant, L. (1997). Simulations for evaluation of kinetic methods in differential scanning calorimetry. Part 3 — Peak maximum evolution methods and isoconversional methods. *Thermochimica Acta,* 293(1), 25-37. https://doi.org/10.1016/S0040-6031(97)00023-3

Sen, Avijit, de Souza, Bernardo, Huntington, Lee M. J., Krupička, Martin, Neese, Frank, & Izsák, Róbert. (2018). An efficient pair natural orbital based configuration interaction scheme for the calculation of open-shell ionization potentials. *The Journal of Chemical Physics, 149*(11). https://doi.org/10.1063/1.5048688

Stoychev, Georgi L., Auer, Alexander A., Izsák, Róbert, & Neese, Frank. (2018). Self-Consistent Field Calculation of Nuclear Magnetic Resonance Chemical Shielding Constants Using Gauge-Including Atomic Orbitals and Approximate Two-Electron Integrals. *Journal of*

Chemical Theory and Computation, *14*(2), 619-637. https://doi.org/10.1021/acs.jctc.7b01006

Stoychev, Georgi L., Auer, Alexander A., & Neese, Frank. (2018). Efficient and Accurate Prediction of Nuclear Magnetic Resonance Shielding Tensors with Double-Hybrid Density Functional Theory. *Journal of Chemical Theory and Computation*, *14*(9), 4756-4771. https://doi.org/10.1021/acs.jctc.8b00624

Thakur, Amit K., Kumar, Rahul, Kumar, Ashutosh, Shankar, Ravi, Khan, Nadeem A., Gupta, Kaushal Naresh, Raj Kumar. (2023). Pharmaceutical waste-water treatment via advanced oxidation based integrated processes: An engineering and economic perspective. *Journal of Water Process Engineering*, *54*, 103977. https://doi.org/10.1016/j.jwpe.2023.103977

Titi, Abderrahim, Badran, Ismail, Dahmani, Mohammed, Messali, Mouslim, Touzani, Rachid, Zarrouk, Abdelkader, . . . Warad, Ismail. (2023). Rapid microwave synthesis of tetrahedral pyrazole/Co(II) complex: [NH···Cl] synthon, XRD/HSA-interactions, DFT/TD-DFT, physiochemical, antifungal, antibacterial, and POM bio-calculations. *Journal of Molecular Structure*, *1293*, 136297. https://doi.org/10.1016/j.molstruc.2023.136297

Vyazovkin, Sergey. (2015). *Isoconversional Kinetics of Thermally Stimulated Processes*. Cham: Springer International Publishing.

Vyazovkin, Sergey, Burnham, Alan K., Criado, José M., Pérez-Maqueda, Luis A., Popescu, Crisan, & Sbirrazzuoli, Nicolas. (2011). ICTAC Kinetics Committee recommendations for performing kinetic computations on thermal analysis data. *Thermochimica Acta*, *520*(1), 1-19. https://doi.org/10.1016/j.tca.2011.03.034

Wang, Jianlong, & Wang, Shizong. (2016). Removal of pharmaceuticals and personal care products (PPCPs) from wastewater: A review. *Journal of Environmental Management*, *182*, 620–640. https://doi.org/doi:10.1016/j.jenvman.2016.07.049

Warad, I. (2021). One-pot ultrasonic synthesis of [Cl(N∩N')Cu(μCl)2Cu(N∩N')Cl] dimer, DFT, XRD/HSA-interactions, spectral, Solvatochromism and TG/DTG/DSC analysis. *Journal of Molecular Structure*, *1236*, 130371. https://doi.org/10.1016/j.molstruc.2021.130371

Warad, I., Musameh, S., Badran, I., et al. (2017). Synthesis, solvatochromism and crystal structure of trans-[Cu($Et_2NCH_2CH_2NH_2$)$_2$.H_2O](NO_3)$_2$ complex: Experimental with DFT combination. *Journal of Molecular Structure*, *1148*, 328-338. https://doi.org/10.1016/j.molstruc.2017.07.067

Wei, Ning, Jia, Lina, Shang, Zeren, Gong, Junbo, Wu, Songgu, Wang, Jingkang, & Tang, Weiwei. (2019). Polymorphism of levofloxacin: structure, properties and phase transformation. *CrystEngComm*, *21*(41), 6196-6207. https://doi.org/10.1039/C9CE00847K

Weigend, F., & Ahlrichs, R. (2005). Balanced basis sets of split valence, triple zeta valence and quadruple zeta valence quality for H to Rn: Design and assessment of accuracy. *Physical Chemistry Chemical Physics*, *7*(18), 3297-3305. https://doi.org/10.1039/B508541A

Worch, Eckhard. (2012). *Adsorption technology in water treatment: fundamentals, processes, and modeling*: Walter de Gruyter.

Yuan, Xinsong, He, Tao, Cao, Hongliang, & Yuan, Qiaoxia. (2017). Cattle manure pyrolysis process: Kinetic and thermodynamic analysis with isoconversional methods. *Renewable Energy*, *107*, 489-496. https://doi.org/10.1016/j.renene.2017.02.026

Zamani-Babgohari, F., Irannejad, A., Khayati, Gholam R., & Kalantari, M. (2023). Non-isothermal decomposition kinetics of commercial polyacrylamide hydrogel using TGA and DSC techniques. *Thermochimica Acta*, *725*, 179532. https://doi.org/10.1016/j.tca.2023.179532

Zhao, Yan, & Truhlar, Donald G. (2008). The M06 suite of density functionals for main group thermochemistry, thermochemical kinetics, noncovalent interactions, excited states, and transition elements: two new functionals and systematic testing of four M06-class functionals and 12 other functionals. *Theoretical Chemistry Accounts*, *120*(1), 215-241. https://doi.org/10.1007/s00214-007-0310-x

Zhou, Zhigao, Zhang, Zhenyan, Feng, Lan, Zhang, Jinfeng, Li, Yan, Lu, Tao, & Qian, Haifeng. (2020). Adverse effects of levofloxacin and oxytetracycline on aquatic microbial communities. *Science of The Total Environment*, *734*, 139499. https://doi.org/10.1016/j.scitotenv.2020.139499